

Theoretical Study on the Assembly and Stabilization of a Magic Cluster Al_4N^-

Li-ming Yang, Yi-hong Ding,* and Chia-chung Sun

State Key Laboratory of Theoretical and Computational Chemistry, Institute of Theoretical Chemistry, Jilin University, Changchun 130023, People's Republic of China

Received: February 7, 2007; In Final Form: June 23, 2007

We report the first attempt to assemble the magic cluster Al_4N^- on the basis of the density functional theory calculations on a series of π -stacked dimers $(\text{Al}_4\text{N}^-)_2$, sandwich-like compounds $[\text{D}(\text{Al}_4\text{N})\text{M}]^{q-}$ (where $\text{D} = \text{Al}_4\text{N}^-$, $\text{Cp}^-(\text{C}_5\text{H}_5^-)$; $\text{M} = \text{Li}, \text{Na}, \text{K}, \text{Be}, \text{Mg}, \text{Ca}$) and extended compounds $(\text{Cp}^-)_m(\text{Li}^+)_n(\text{Al}_4\text{N}^-)_o$ (where m , n , and o are integers). For the six metals, the magic Al_4N^- can only be assembled and grow up in our newly proposed “hetero-decked sandwich” scheme (e.g., $[\text{CpM}(\text{Al}_4\text{N})]^{q-}$) so as to avoid cluster fusion. The ground-state hetero-decked sandwich species $(\text{Cp}^-)(\text{M})^{q+}(\text{Al}_4\text{N}^-)$ ($\text{M} = \text{Li}, \text{Na}, \text{K}, q = 1$; $\text{M} = \text{Be}, \text{Mg}, \text{Ca}, q = 2$) and the extended sandwich species $(\text{Cp}^-)_m(\text{Li}^+)_n(\text{Al}_4\text{N}^-)_o$ are mainly ionically bonded, cluster-assembled “polyatomic molecules”, grown from the combination of Cp^- , M-atoms, and Al_4N^- . As a prototype for ionic bonding involving intact Al_4N^- subunits, $[\text{CpM}(\text{Al}_4\text{N})]^{q-}$ may be a stepping stone toward forming ionic, cluster-assembled AlN compounds.

1. Introduction

The chemistry and industry of aluminum nitride (AlN)^{1–5} have attracted considerable attention due to its joint functions among material science^{1–4} and nanoscience/technology (AlN fullerenes and nanotubes)² and its wide applications in semiconductors³ and ceramics.⁴ Small aluminum nitride clusters have been the subject of extensive studies over the past two decades.⁵ A large number of aluminum nitride clusters have been probed experimentally. Additionally, the discovery of fullerenes (C_{60})⁶ (and the subsequent preparation in bulk quantities), metcars (M_8C_{12}),⁷ and Al_{13}^{8a-c} have inspired speculation that it might be possible to form macroscopic samples without coalescing with one another and losing their individual identities. Although, AlN chemistry has undergone vast development, a huge gap still exists between the small building blocks and the bulk solid compounds. How can the small units grow up into cluster-assembled bulk species? Elucidating the growth mechanism will shed insight on designing novel AlN compounds.

Currently, one promising concept that has emerged is the possibility of creating new compounds using atomic or compound clusters as the building blocks, as was previously discussed by Khanna and Jena^{8d,e} and by Kaya and co-workers.^{8f} If possible, this would bring the level of atomic control realized in the properties of clusters to the design of compounds with desirable collective traits. Generally, building blocks that are used for cluster-assembled compounds are highly stable closed-shell species, for example, fullerenes, metcars, magic clusters, and superatoms. The magic-numbered unit Al_4N^{5-} (D_{4h}) cluster forms the focus of our study due to its particularity. It is one of the simplest and the first experimentally known planar tetra-coordinate nitrogen (ptN) species. It contains a beautiful square structure with a central nitrogen in planar tetracoordination. Utilization of such an exotic magic unit as a building block might be of great interest. Yet the fundamental issue is the following: (1) Can Al_4N^- be used for cluster assembly? (2) If

this is possible, how can the magic cluster Al_4N^- be assembled and stabilized? “Bottom-up” gives us the answer!

Herein, we explore the bottom-up growth of the relatively simple and magic-numbered Al_4N^- , which is experimentally available and possesses unique properties, that is, high-symmetry, aromaticity,⁹ planarity, and simplicity. We considered an important strategy—“sandwiching”, which is probably the most powerful one for assembly and growth of a stable small unit (e.g., C_5H_5^- (Cp^-)) into more complex compounds and has gestated in a rich chemistry of metallocenes (CpMCp).^{10a} We made the first attempt to design the π -stacked dimers and the assembled systems in sandwich-like forms based on the magic unit Al_4N^- . We found that the π -stacked growth pattern is not feasible, and for all six metals ($\text{M} = \text{Li}, \text{Na}, \text{K}, \text{Be}, \text{Mg}$, and Ca) the assembly and growth of Al_4N^- cannot be realized in the traditional “homo-decked sandwich” form $[(\text{Al}_4\text{N})_2\text{M}]^{q-}$. However, our newly proposed “hetero-decked sandwich”^{10b-e} scheme (e.g., $[\text{CpM}(\text{Al}_4\text{N})]^{q-}$) is very effective in assembly and growth. The good structural and electronic integrity of the Al_4N^- unit within the designed assembled systems leads us to propose that the magic unit Al_4N^- might act as a new kind of “superatom”^{8d-f,11} in combinational chemistry.

2. Computational Methods

Initially, we fully optimized the geometries of $[\text{D}(\text{Al}_4\text{N})\text{M}]^{q-}$ ($\text{D} = \text{Al}_4\text{N}^-$, Cp^- ; $\text{M} = \text{Li}, \text{Na}, \text{K}, q = 1$; $\text{M} = \text{Be}, \text{Mg}, \text{Ca}, q = 0$) employing analytical gradients with the polarized split-valence basis set 6-311+G(d) using the hybrid method, which includes a mixture of Hartree–Fock exchange with density functional exchange correlation (B3LYP).^{13a-d} After geometrical optimization, vibrational analyses were performed to check whether the obtained structures are local minima with all real frequencies. All calculations were performed with the Gaussian-03 program (see ref 13e and the Supporting Information section).

3. Theoretical Results and Discussions

A. Can Al_4N^- Grow Up in the Bricklaying Architecture?

The high-symmetry of magic cluster Al_4N^- inspired us to

* Corresponding author. Fax: +86-431-88498026. E-mail: yhdd@mail.jlu.edu.cn.

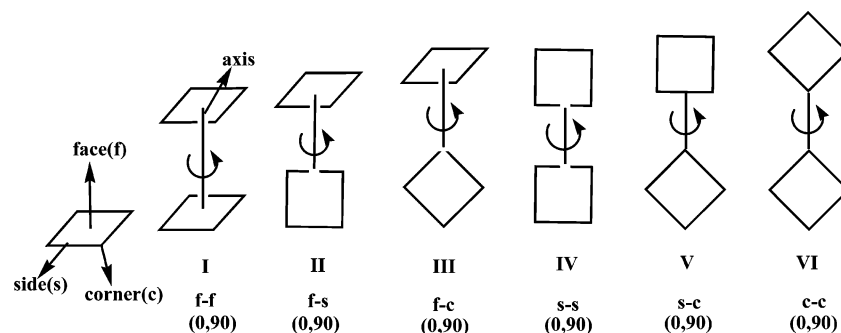


Figure 1. Six possible interaction types of $[(\text{Al}_4\text{N})_2]^{2-}$ (I–VI). For simplicity, the center N-atom is omitted. In each type, one unit can rotate along the axis by 0° and 90° .

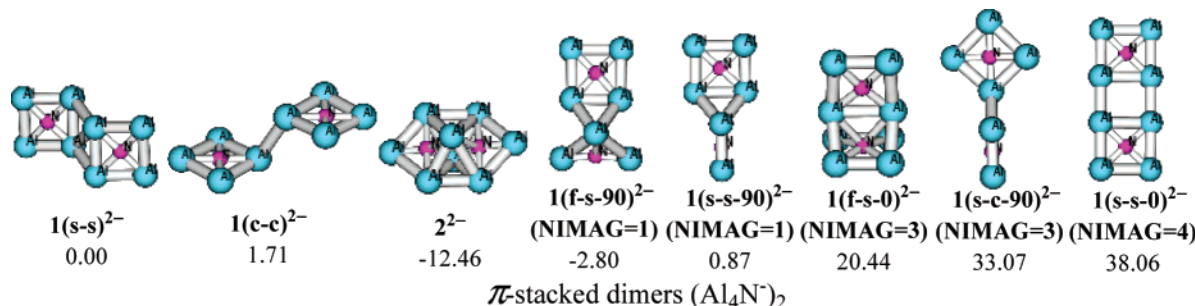


Figure 2. Most relevant $[\text{Al}_8\text{N}_2]^{2-}$ species at the B3LYP/6-311+G(d) level. The energy values are in kcal/mol.

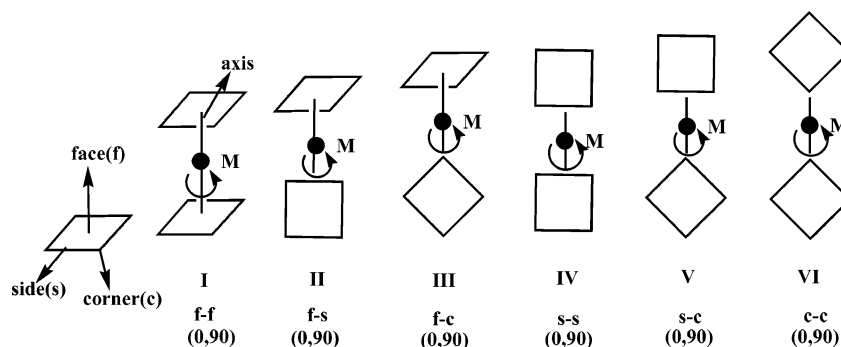


Figure 3. Six possible sandwich types of $[(\text{Al}_4\text{N})_2\text{M}]^{q-}$ (I–VI) for each M. For simplicity, the center N-atom is omitted. In each type, one unit can rotate along the axis by 0° and 90° .

wonder whether such a beautiful building block can be self-assembled like C_{60} .⁶ The aromaticity⁹ of Al_4N^- hints that it might grow up and be stabilized in the form of the analog of benzene π -stacking interactions (benzene dimer interactions),^{12a–b} which have been stressed in many fields ranging from molecular biology¹² to material sciences.¹² Thus, it would be very interesting to investigate whether magic Al_4N^- can also form π -stacked dimers, trimers, and even oligomers and polymers. We consider various interaction types (Figure 1) between two Al_4N^- units in the combination of f (face), s (side), and c (corner) directions. After a detailed structural search at the B3LYP/6-311+G(d)¹³ level, we found that all the structural types shown in Figure 1 are not energy minima. Instead, many agglomeration forms have lower energies (see Figure 2). (All the energy profiles of the $[\text{Al}_8\text{N}_2]^{2-}$ species can be found in the Supporting Information section.) Thus, the magic cluster Al_4N^- cannot “grow up” in the self-organized assemblies without any other help.

B. Can Metal Atoms Effectively Separate and Protect the Magic Al_4N^- Decks? The failure of the direct layered self-assembly of Al_4N^- described in Section A prompts us to inspect the possibility of the Al_4N^- self-assembly assisted by M-atoms. Here, M- atoms may play two important roles in cluster self-

assembly grown-up processes, that is, isolate and charge-compensate two or more Al_4N^- units. The assembly of the magic Al_4N^- in the traditional “homo-decked sandwich” form $[(\text{Al}_4\text{N})_2\text{M}]^{q-}$ with $\text{M} = \text{Li}, \text{Na}, \text{K}, q = 1$; $\text{M} = \text{Be}, \text{Mg}, \text{Ca}, q = 0$ is investigated at the B3LYP/6-311+G(d) level. The possible sandwich interaction types are shown in Figure 3. The type I structure is similar to the well-known metallocene CpMCP , in which two Cp^- adopt the face–face (f–f) type. The energy profiles of the most relevant $[\text{Al}_8\text{N}_2\text{M}]^{q-}$ species, that is, all sandwich forms and those with lower energy than the lowest-energy sandwich form, are schematically shown in Figure 4. The other isomers can be found in Supporting Information. First, for all the six main-group elements, the sandwich species IV–VI have energies that are very close to each other and are all energetically lower than I–III. Via the rotation of the Al_4N deck along different axes, I–III can be easily converted to the lower-energy IV–VI. The interconversion between IV–VI via simple rotation is also very easy, as can be indicated by the very small rotation frequency. Second, there are many fusion isomers lower than the lowest-energy sandwich structure and it is thus thermodynamically unstable. Thus, the magic-numbered Al_4N^- cannot be assembled or grown up in the “homo-decked sandwich” growth pattern. This might

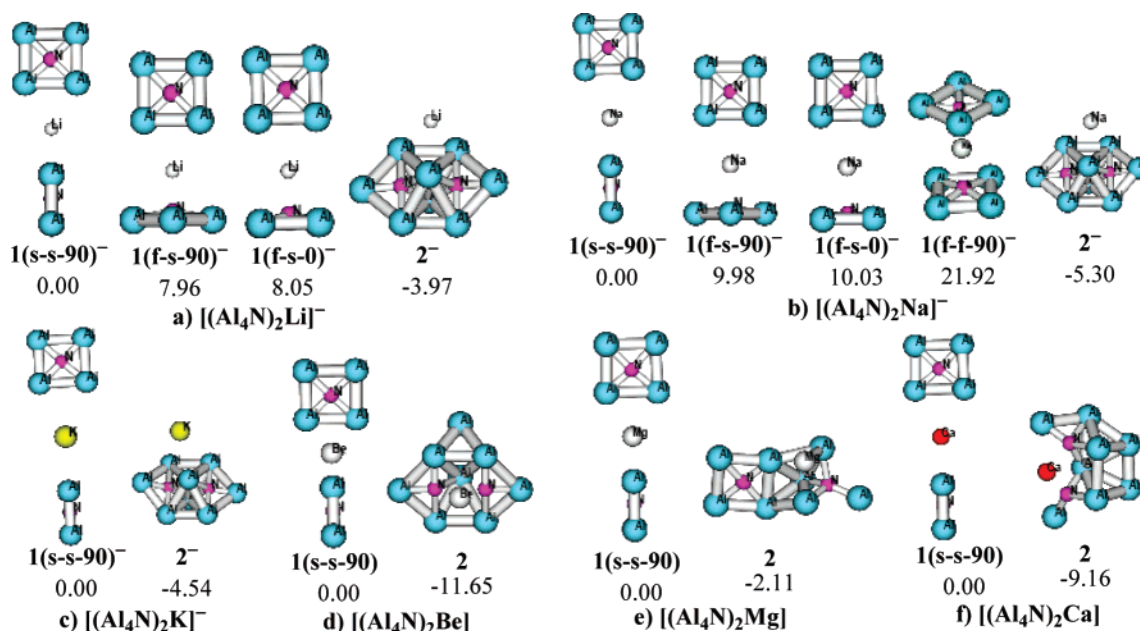


Figure 4. Most relevant $[\text{Al}_8\text{N}_2\text{M}]^{q-}$ ($\text{M} = \text{Li}, \text{Na}, \text{K}, q = 1$; $\text{M} = \text{Be}, \text{Mg}, \text{Ca}, q = 0$) species at the B3LYP/6-311+G(d) level. The energy values are in kcal/mol.

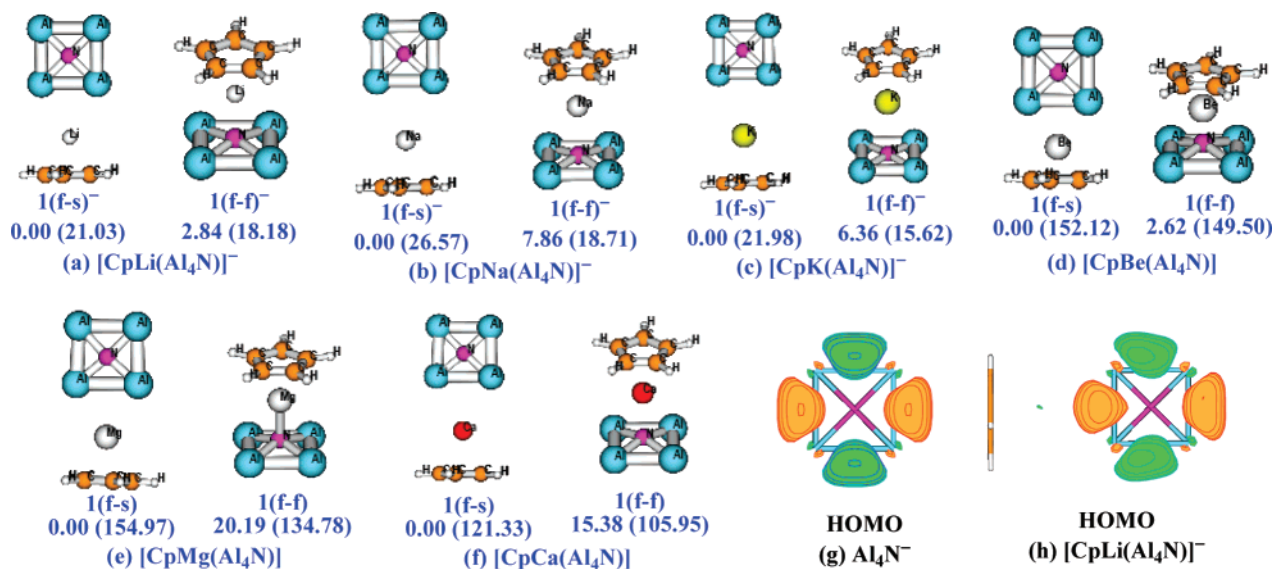


Figure 5. The sandwich forms of $[\text{CpM}(\text{Al}_4\text{N})]^{q-}$ ($\text{M} = \text{Li}, \text{Na}, \text{K}, q = 1$; $\text{M} = \text{Be}, \text{Mg}, \text{Ca}, q = 0$) obtained at the B3LYP/6-311+G(d) level. Relative energy and binding energy (in parentheses) between the Al_4N^- unit and fragment CpM^{q+} are listed. Energy values are in kcal/mol. The B3LYP/6-311+G(d) orbital diagrams^{12f} of (g) Al_4N^- and (h) $[\text{CpLi}(\text{Al}_4\text{N})]^-$.

be ascribed to the fusion trend between the two Al_4N^- decks and that the M-atoms cannot effectively separate the Al_4N^- units in the array.

C. Cooperation of Metal Atoms with the Organic Aromatic Deck Cp^- (C_5H_5^-) Can Effectively Separate and Protect the Magic Al_4N^- . Section B told us that the magic Al_4N^- still cannot grow up solely assisted by M-atoms in the “homo-decked sandwich” form. Additional assistance and other stabilization factors are necessary in the growth of Al_4N^- . Here we show that an isolation-wall like the rigid and organic aromatic deck Cp^- can cooperate with the magic-numbered Al_4N^- to sandwich the M-atoms by avoidance of fusion in the growth process. Various isomeric forms for each of the six main-group elements ($\text{M} = \text{Li}, \text{Na}, \text{K}, \text{Be}, \text{Mg}$, and Ca) are searched. For simplicity, only the lower-lying structures are shown in Figure 5. Others can be found in Supporting Information. For all the six metals ($\text{M} = \text{Li}, \text{Na}, \text{K}, \text{Be}, \text{Mg}$, and Ca), two kinds of sandwich forms $1^{q-}(\text{f-s})$ and $1^{q-}(\text{f-f})$ exist, with the former

associated with the “face (Cp^-)–side (Al_4N^-)” (f-s) type and the latter with the “face (Cp^-)–face (Al_4N^-)” (f-f) type. The scheme described here is called “hetero-decked sandwich”, which has been successfully applied to the sandwiching of the all-metal aromatic units Al_3^{2-} ^{10b} and Al_4^{2-} ^{10c} as well as the planar tetracoordinate carbon units CAu_4^{2-} ^{10d} and Al_3Si^- .^{10e} In this way, the magic units Al_4N^- can be effectively separated and protected. The designed species $[\text{CpM}(\text{Al}_4\text{N})]^{q-}$ belong to a new class of sandwich-like compounds, which are intuitively of special interest because they contain both the classic organic aromatic unit Cp^- and the novel magic unit Al_4N^- . In order to evaluate the stabilities of our designed hetero-decked sandwich-type complexes, we made calculations on the binding energies between the magic cluster Al_4N^- and fragments CpM^{q+} for the hetero-decked sandwich species $[\text{CpM}(\text{Al}_4\text{N})]^{q-}$. For alkali metals $\text{M} = \text{Li}, \text{Na}$, and K , the binding energies are about 20 kcal/mol (see Figure 5). For alkaline earth metals $\text{M} = \text{Be}, \text{Mg}$, and Ca , the binding energies range from 105 to 155 kcal/

mol. Note that the binding energies are large for the alkaline earth metals, mainly due to the coulomb interactions. The above binding energies are indicative of sufficient stability of our designed hetero-decked assembled compounds.

Interestingly, among all the designed homo-decked and hetero-decked sandwich species, the magic Al_4N^- generally prefers to use its side (Al–Al bond) site to interact with the partner deck Al_4N^- or Cp^- . This is in contrast to the known decks such as the famous and versatile Cp^- and the carbon-free and exotic Al_4^{2-} ,^{14a–b} $\text{P}_3^{14c–e}$ and N_4^{2-} ,^{14f–i} that prefer the traditional face–face (f–f) interaction type. Moreover, among all the calculated $[\text{CpM}(\text{Al}_4\text{N})]^{q-}$ systems, the planar Cp^- structure is well maintained, indicative of the unique “rigidity” of this organic unit. Fusion of the Cp^- and Al_4N^- decks to form new C–Al, C–N, or C–M bonds is energetically unfavorable. This indicates that Al_4N^- can be viewed as a “superatom”. The Al_4N^- can grow up into dimer, trimer, oligomer, and even polymer in the form of the hetero-decked packing through M-atoms lying between Cp^- and Al_4N^- . The Al_4N^- , M-atoms, and Cp^- alternant position in the array should be ideal arrangements in designing more complex compounds based on the magic Al_4N^- .

In order to get insight into the origin of planarity and exotic electronic structure of such novel sandwich-like compounds based on the magic Al_4N^- , we examined the molecular orbitals of bare Al_4N^- and the sandwich-like compound $[\text{CpLi}(\text{Al}_4\text{N})]^-$. Figure 5g,h shows their highest occupied molecular orbitals (HOMOs): the ligand–ligand bonding HOMO. The structural planarity of these species is achieved through a strong four-center peripheral ligand–ligand bonding interaction in their highest occupied molecular orbital (HOMO). From Figure 5g,h we can see the shapes of orbitals in (g) bare Al_4N^- and (h) sandwich-like compound $[\text{CpLi}(\text{Al}_4\text{N})]^-$ are generally the same. Thus, the magic Al_4N^- can maintain its electronic and structural integrity in sandwich forms. Therefore, Al_4N^- could be used as a building block and “superatom” in designing planar tetracoordinate nitrogen complexes and planar AlN compounds. The originality of planarity of other simple pentatomic species has been previously revealed in several nice papers.^{5a–i}

In order to get insight into the interactions of our designed hetero-decked sandwich-type complexes, we perform detailed NBO^{16a–c} analysis. The NPA charges on the Al_4N units range from -0.901 to -1.009 |e|, from -0.923 to -0.981 |e|, from -0.964 to -0.992 |e|, from -0.386 to -0.918 |e|, from -0.545 to -0.926 |e|, and from -0.793 to -0.894 |e| in the hetero-decked sandwich-like compounds $[\text{CpM}(\text{Al}_4\text{N})]^{q-}$ for $\text{M} = \text{Li}$, Na , K , Be , Mg , and Ca , respectively. Generally, the NPA charges on Al_4N units in the alkali metal sandwich species are very close to that of the free Al_4N^- (ionic limit of -1). Whereas the NPA charges on Al_4N units in the alkaline earth metal sandwich species are a slight departure from that of the free Al_4N^- . For $\text{M} = \text{Be}$, the departure is slightly larger due to its large covalent property. The NPA charges on the Cp units range from -0.856 to -0.905 |e|, from -0.919 to -0.944 |e|, from -0.956 to -0.961 |e|, from -0.758 to -0.770 |e|, from -0.840 to -0.856 |e|, and from -0.851 to -0.859 |e| in $[\text{CpM}(\text{Al}_4\text{N})]^{q-}$ for $\text{M} = \text{Li}$, Na , K , Be , Mg , and Ca , respectively. Thus, the NPA charges on the Cp units are close to that of the free Cp^- . The NPA charges on alkali metal atoms (Li , Na , and K) range from $+0.806$ to $+0.865$ |e|, from $+0.866$ to $+0.900$ |e|, and from $+0.926$ to $+0.948$ |e| in $[\text{CpM}(\text{Al}_4\text{N})]^-$ for $\text{M} = \text{Li}$, Na , and K , respectively. For the alkaline earth atoms, the NPA charges range from $+1.156$ to $+1.676$ |e|, from $+1.401$ to $+1.766$ |e|, and from $+1.652$ to $+1.745$ |e| in $[\text{CpM}(\text{Al}_4\text{N})]$

for $\text{M} = \text{Be}$, Mg , and Ca , respectively. We can see that the NPA charges on alkali metal atoms (Li , Na , and K) are a slight departure from the ionic limit of $+1$. For alkaline earth atoms (Be , Mg , and Ca), the NPA charges are a slight departure from the ionic limit of $+2$, whereas for Be , the departure is slightly larger due to its large covalent property.

Additional evidence of the stability of the hetero-decked assembled species comes from an inspection of the energy of the following reaction: $\text{Cp}^- + \text{M}^{n+} + \text{Al}_4\text{N}^- \rightarrow [\text{CpM}(\text{Al}_4\text{N})]^{q-}$ ($\text{M} = \text{Li}$, Na , K , $n = q = 1$; $\text{M} = \text{Be}$, Mg , Ca , $n = 2$, $q = 0$). The heat of formation of the hetero-decked species $[\text{CpM}(\text{Al}_4\text{N})]^{q-}$ range from -190.05 to -192.90 , from -166.58 to -158.72 , from -145.04 to -138.68 , from -676.66 to -674.03 , from -531.24 to -511.05 , and from -443.78 to -428.40 kcal/mol for $\text{M} = \text{Li}$, Na , K , Be , Mg , and Ca , respectively. The above synthesis reactions release large energies, thus indicative of the strongly thermodynamical feasibility. We are aware that the cohesive energies between the dication (M^{2+}) and the monoanions (Cp^- and Al_4N^-) are much larger than the cohesive energies between the monocation (M^+) and monoanions (Cp^- and Al_4N^-). Such results are consistent with the theorem of electrostatics. The fragmentation of the hetero-decked sandwich species will not occur easily, because the cohesive energies are large.

D. Origin of Fusion. Why can the assembly of Al_4N^- only be realized in the form of the “hetero-decked sandwich” scheme instead of the π -stacked growth pattern or the traditional “homo-decked sandwich” scheme? Why would the π -stacked growth pattern and the “homo-decked sandwich” assembly lead to fusion between two Al_4N^- decks? To answer these questions, let us analyze the mechanism of cluster assembly.

Two types of reaction processes might take place when the decks D_1^{m-} , D_2^{n-} , and one M^{q+} ion come close:

- (1) **ionic interaction:** $\text{D}_1^{m-} + \text{M}^{q+} + \text{D}_2^{n-} \rightarrow (\text{D}_1^{m-})\text{M}^{q+}(\text{D}_2^{n-})$
- (2) **fusion interaction:** $\text{D}_1^{m-} + \text{D}_2^{n-} + \text{M}^{q+} \rightarrow \text{M}^{q+}[\text{D}_1\text{D}_2]^{(m+n)-}$

In process (1), each sandwiching deck (D_1^{m-} and D_2^{n-}) participates in the electrostatic interaction with M^{q+} to form a sandwich-like structure $(\text{D}_1^{m-})\text{M}^{q+}(\text{D}_2^{n-})$. In process (2), the “clustering fusion” takes place. Principally, any two decks have the trend to form a more coagulated cluster containing more bonds so as to lower the system energy. The competition between processes (1) and (2) determines whether formation of a sandwich-like complex or a coagulated cluster leads to energetic stabilization. When the monoanionic Al_4N^- undergoes the traditional “homo-decked sandwich” assembly, the fusion interaction overwhelms the ionic interaction because of the favorable cluster coagulation. The bonding within the magic Al_4N^- is not strong enough to avoid fusion. So, as shown in section A, the homo-decked sandwich structures are energetically much less stable than the fused isomers. Yet, the situation is quite different in the novel “hetero-decked sandwich” form. The fusion tendency can be greatly suppressed due to the introduction of a rigid sandwiching partner Cp^- . The large organic aromaticity allows Cp^- to perfectly keep its (near) D_{5h} structure. Any structural fusion with Al_4N^- will destroy the aromaticity of Cp^- to greatly raise the system energy. As a result, only in the form of the novel “hetero-decked sandwich” scheme can the magic Al_4N^- be assembled into sandwich-like complexes.

The above detailed analysis of the ionic and clustering interactions between the two decks is quite crucial to improve the insight and cognition on the nature and origin of the interactions of the “deck–core–deck” in the metallocenes. Such information is also important in understanding and designing

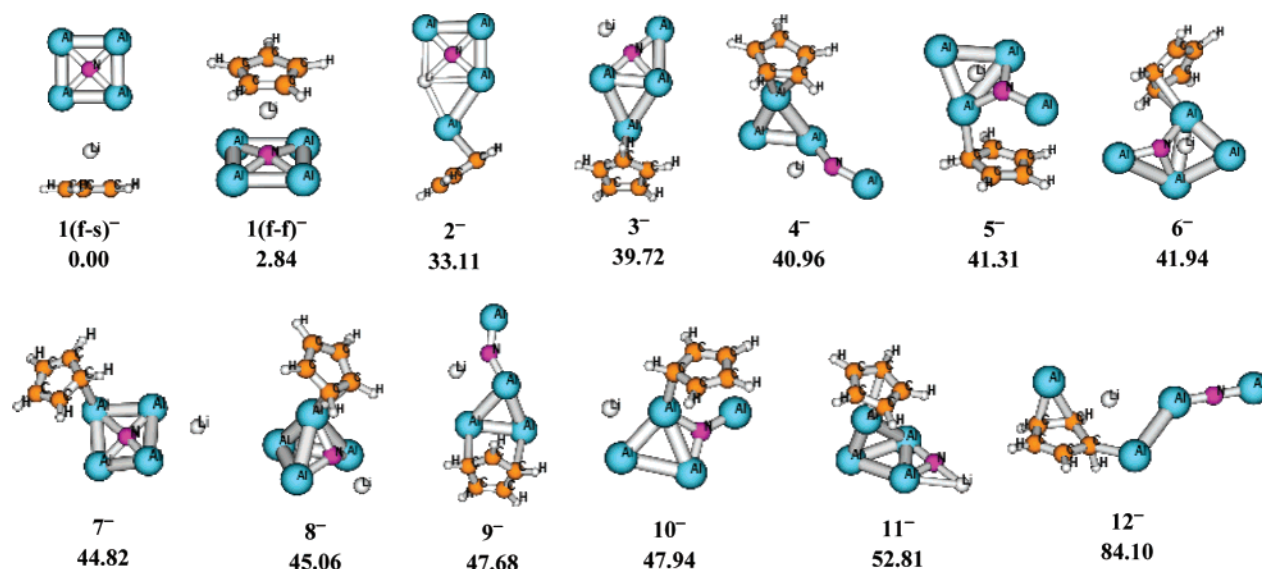


Figure 6. Some illustrative comparative structures of sandwich-like and fusion isomers of hetero-decked sandwich-like complexes $[\text{CpLi}(\text{Al}_4\text{N})]^-$ are obtained at the B3LYP/6-311+G(d) level, the energy values are in kcal/mol.

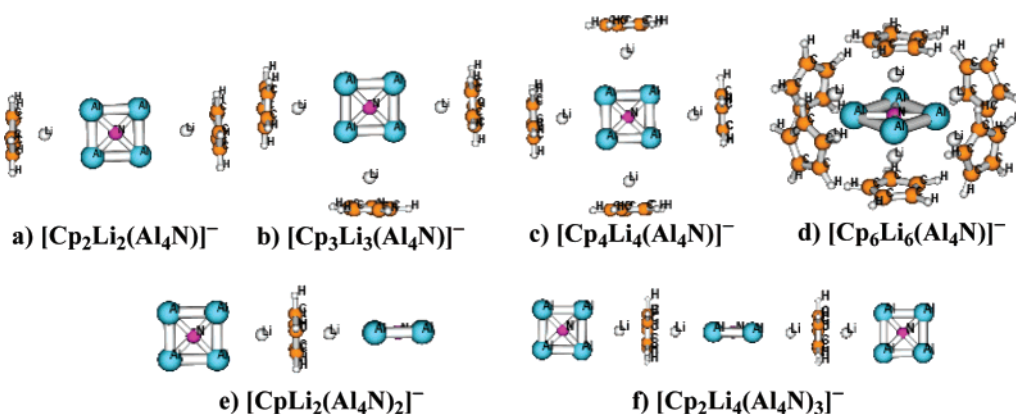


Figure 7. Selected extended sandwich complexes obtained at the B3LYP/6-31+G(d) level.

novel sandwich-type complexes and cluster-assembled molecular compounds. For intuitionistic understanding of the above discussion, we illustrate the comparative structures of sandwich-like species and fusion isomers of hetero-decked assembled complexes $[\text{CpLi}(\text{Al}_4\text{N})]^-$ in testimony of the above analysis. The Cp^- and Al_4N^-9 are two aromatic decks, any of which distorted or fused together will reduce or even destroy the aromaticity and thus lead to high energies. From Figure 6, we can see that the fusion isomers are indeed energetically higher than sandwich-like forms.

Also, we can make an energetic estimate for the loss of aromaticity from the comparison of the low-lying sandwich species and high-lying fusion isomers. In Figure 6, the aromaticity of the two aromatic decks Cp^- and Al_4N^-9 is reduced or even largely destroyed in the fusion isomers (2⁻–12⁻). From isomers 2⁻–11⁻, the aromaticity of Al_4N^- is almost destroyed, and the aromaticity of Cp^- is reduced or partially destroyed. In isomer 12⁻, the aromaticity of Al_4N^- is completely destroyed, and the aromaticity of Cp^- is almost destroyed, that is, the two aromatic decks are all destroyed, indicative that the average energy of the simultaneous loss of aromaticity of Cp^- and Al_4N^- is more than 80 kcal/mol. So, the fusion isomer 12⁻ is energetically much higher than the other fusion isomers (2⁻–11⁻). Thus, the average energy for the loss of aromaticity of Al_4N^- is about 40 kcal/mol, which can be estimated from the comparison between sandwich isomer 1⁻ and fusion isomers (2⁻–11⁻). The average energy for the loss of aromaticity of

Cp^- is about 50 kcal/mol, which can be estimated from the comparison between the fusion isomers 2⁻ and 12⁻. It should be pointed out that the above estimate of average energy for the loss of the aromaticity is qualitative. In summary, the fusion isomers are energetically much higher than the sandwich species. Moreover, the aromaticity of the fusion isomers is reduced, partially destroyed, or even completely destroyed compared with that of the sandwich species.

E. Magic Al_4N^- Grows Up in the Extended Sandwich-like Structures. Can magic Al_4N^- form extended sandwich compounds? From the preceding discussions, we have confidence that the hetero-decked sandwich scheme is an effective growth pattern for magic Al_4N^- . The high symmetry of Al_4N^- and the f-s, f-c, and f-f interaction types render the “bottom-up” growth very promising! As an extension of the present study and a testimony of “bottom-up” growth, we design the Al_4N^- -based extended systems containing more Cp^- and Al_4N^- units in various sandwich-like forms at the B3LYP/6-31+G(d) level. For simplicity, only selected low-lying species are shown in Figure 7. We can easily see the atomic-level manipulation and assembly of the magic Al_4N^- as well as the isolation effects of Cp^- . Many other designed extended sandwich-like structures can be found in Supporting Information. Surely, the growth mechanism from the simple extended sandwich-like structures (Figure 7) to the much more highly extended 3D sandwich-like species with more Cp^- and Al_4N^- units $(\text{Cp}^-)_m(\text{Li}^+)_n(\text{Al}_4\text{N}^-)_o$ (m , n , and o are integers) is viable. Because of computational

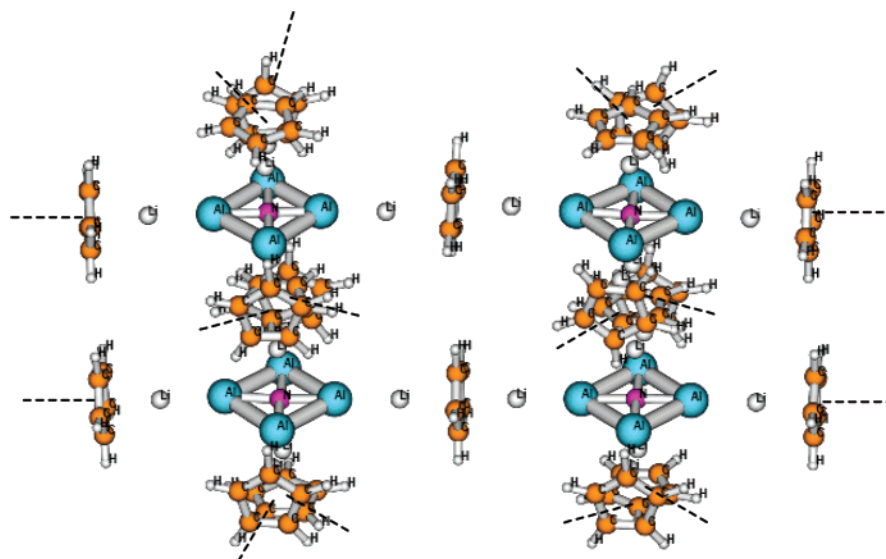


Figure 8. Illustrative more highly extended 3D sandwich structure based on Al_4N^- . The dashed lines show the cluster-growth direction in which more Al_4N^- or Cp^- decks can be added.

cost, we do not attempt to calculate these species. One illustrative example is given in Figure 8.

F. A General and Effective Growth Pattern of Magic Al_4N^- Cluster: Capture, Assembly, and Stabilization of the Magic Al_4N^- Cluster through a Separated and Protected Scheme.

The capture, assembly, and stabilization of a stable cluster have continued to be a hot topic for chemists. Similar to the recently discovered Au_{20} ,¹⁵ the magic Al_4N^- still needs protection in its assembly and growth processes. Generally, the protection and stabilization of a unique cluster have to be made by using bulky substitutions within the molecular skeleton (e.g., PPh_3 , $\text{C}(\text{CH}_3)_3$). Yet, a severe shortcoming of such “steric-stabilization” is that it is difficult to modify and grow further. Moreover, they cannot be used as building blocks in cluster assembly due to the steric effects. The natural bond orbital (NBO)^{16a-c} analyses can give new insights into the understanding of the atomic charge distribution of Al_4N^- -based sandwich species. The NBO results^{16d} indicate that in the free Al_4N^- and Al_4N^- -based sandwich-like species, the N atom serves as the negatively charged nonmetal center and the four peripheral Al atoms form a positively charged ring. This suggests that each of the peripheral atoms is apt to react with outer reagents. Luckily, our newly proposed “hetero-decked sandwich” scheme can effectively suppress the reactivity of Al_4N^- by introducing the LiCp pairs (see Figure 5 and 7). It is even possible that the reactivity of Al_4N^- can be completely suppressed by being fully “dressed” with six LiCp pairs (see Figure 7d) in six directions. In this way, the magic Al_4N^- is well captured into a “rice-ball” structure (Figure 7c) and a “cage” structure (Figure 7d). We call such a cluster-stabilization method “sandwich-stabilization”. The advantage of the new method is that (1) the steric effect can easily be introduced by choosing suitable “dressers” (e.g., change LiCp to LiCp* with all hydrogen atoms substituted by methyl groups); (2) since the bonding between Al_4N^- and the LiCp pair is mainly of the ionic interaction, the neutral LiCp pair can easily be “undressed” when we want to have Al_4N^- for further usage; and (3) thus, the manipulation of cluster size should be easy by simply capturing more Al_4N^- units dressed by LiCp pairs. The new method may present an effective way to control and modulate the properties of target cluster-assembled molecular complexes.

The easy capturability by our newly proposed “hetero-decked sandwich” scheme and the electronic and structural-embedded

“superatom” feature lead us to predict that the magic Al_4N^- can act as a robust building block to design novel molecular compounds. We believe that the properties of the designed sandwich-like compounds should depend on the number of magic number Al_4N^- . The bulky LiCp pairs should well separate the Al_4N^- -decks from each other, resulting in the effective avoidance of fusion. Thus, our designed “hetero-decked sandwich” and proposed nanoscale highly extended sandwich-like species would be ideal candidates for promising nanoscale devices.

4. Conclusions

In summary, the present study described the first attempt to assemble and stabilize the magic unit Al_4N^- into assembled molecular systems in sandwich-like forms. The growth pattern of magic Al_4N^- is apt to take the f-s and f-f interaction forms, which are favorable in avoiding cluster fusion under the isolation effects. The designed species await future experimental verification (e.g., anion photoelectron spectroscopy and solution synthesis). Current studies suggest that it is possible to synthesize “cluster-salt crystals” of our predicted AlN species. Such assembly procedures could also be applied to many other ptN molecules (Al_xN^- ($x = 3, 5$), Al_3SiN) and ptC species (AlSi_3B , CAI_3Ge , CAI_3Ge^- , CSi_2X_2 ($\text{X} = \text{Al, Ga}$) and $\text{CGe}_2\text{-Al}_2$). Compared to the traditional metallocenes with mere Cp^- decks, our designed complexes represent a new class of metallocene containing the magic cluster Al_4N^- , among which Al_4N^- generally prefers to use its side (Al–Al bond) to interact with the partner deck rather than in form of the traditional face–face interaction type for the known decks Cp^- , P_5^- , Al_4^{2-} , and N_4^{2-} . Moreover, the structural and electronic integrity of Al_4N^- are generally well kept during the hetero-decked sandwiching. Thus, Al_4N^- could act as a new type of “superatom”. To our knowledge, this is the first time to propose a planar nitrogen-doped aluminum cluster as a superatom. Future studies on the “superatom” chemistry of Al_4N^- are desired.

Acknowledgment. This work is supported by the National Natural Science Foundation of China (No. 20103003, 20573046), Excellent Young Teacher Foundation of Ministry of Education of China’s Excellent Young People Foundation of Jilin Province,

and Program for New Century Excellent Talents in University (NCET). The reviewer's invaluable comments are greatly appreciated.

Supporting Information Available: Full ref 13e. Structures and calculated properties of molecules. This information is available free of charge via the Internet at <http://pubs.acs.org>.

References and Notes

- (1) (a) Ponce, F. A.; Bour, D. P. *Nature (London)* **1997**, *386*, 351. (b) Kiehne, G. T.; Wong, G. K. L.; Ketterson, J. B. *J. Appl. Phys.* **1998**, *84*, 5922. (c) Krupitskaya, R. Y.; Auner, G. W. *J. Appl. Phys.* **1998**, *84*, 2861. (d) Kuo, P. K.; Auner, G. W.; Wu, Z. L. *Thin Solid Films* **1994**, *253*, 223. (e) Ruiz, E.; Alvarez, S.; Alemany, P. *Phys. Rev. B* **1994**, *49*, 7115. (f) Wang, X. D.; Jiang, W.; Norton, M. G.; Hips, K. W. *Thin Solid Films* **1994**, *251*, 121. (g) Kotula, P. G.; Carter, C. B.; Norton, M. G. *J. Mater. Sci. Lett.* **1994**, *13*, 1275. (h) Rille, E.; Zarwasch, R.; Pulker, H. K. *Thin Solid Films* **1993**, *228*, 215. (i) Kim, H. J.; Egashira, Y.; Komiyama, H. *Appl. Phys. Lett.* **1991**, *59*, 2521. (j) Pauleau, Y.; Bouteville, A.; Hantzpergue, J. J.; Remy, J. C.; Cachard, A. *J. Electrochem. Soc.* **1980**, *127*, 1532. (k) Kimura, I.; Hotta, N.; Nukui, H.; Saito, N.; Yasukawa, S. *J. Mater. Sci. Lett.* **1988**, *7*, 66. (l) Kimura, I.; Hotta, N.; Nukui, H.; Saito, N.; Yasukawa, S. *J. Mater. Sci.* **1989**, *24*, 4076. (m) Egashira, Y.; Kim, H. J.; Komiyama, H. *J. Am. Ceram. Soc.* **1994**, *77*, 2009. (n) Hashman, T. W.; Pratsinis, S. E. *J. Am. Ceram. Soc.* **1992**, *75*, 920. (o) Lee, W. Y.; Lackey, W. J.; Agrawal, P. K. *J. Am. Ceram. Soc.* **1991**, *74*, 1821. (p) Chu, T. L.; Kelm, R. P. *J. Electrochem. Soc.* **1975**, *122*, 995. (q) Jiang, Z. P.; Interrante, L. V. *Chem. Mater.* **1990**, *2*, 439. (r) Sauls, F. C.; Interrante, L. V. *Coord. Chem. Rev.* **1993**, *128*, 193. (s) Sauls, F.; Interrante, L. V.; Jiang, Z. P. *Inorg. Chem.* **1990**, *29*, 2989. (t) Sauls, F. C.; Hurley, W. J.; Interrante, L. V.; Marchetti, P. S.; Maciel, G. E. *Chem. Mater.* **1995**, *7*, 1361.
- (2) (a) Wu, Q.; Hu, Z.; Wang, X. Z.; Lu, Y. N.; Chen, X.; Xu, H.; Chen, Y. *J. Am. Chem. Soc.* **2003**, *125*, 10176–10177. (b) Zhao, M. W.; Xia, Y. Y.; Zhang, D. J.; Mei, L. M. *Phys. Rev. B* **2003**, *68*, 235415. (c) Chen, X.; Ma, J.; Hu, Z.; Wu, Q.; Chen, Y. *J. Am. Chem. Soc.* **2005**, *127*, 7982–7983, and references therein. (d) Xu, X. H.; Wu, H. S.; Zhang, F. Q.; Zhang, C. J.; Jin, Z. H. *J. Mol. Struct.: THEOCHEM* **2001**, *542*, 239. (e) Zhang, D. J.; Zhang, R. Q. *Chem. Phys. Lett.* **2003**, *371*, 426. (f) Wu, H. S.; Zhang, F. Q.; Xu, X. H.; Zhang, C. J.; Jiao, H. J. *J. Phys. Chem. A* **2003**, *107*, 204–209.
- (3) (a) Nakamura, S. In *Proceedings of International Symposium on Blue Laser and Light Emitting Diodes*; Yoshikawa, A., Kishino, K., Klobayashi, M., Yasuda, T., Eds.; Chiba University Press: Chiba City, 1996; p 119, and references therein. (b) Belyanin, A. F.; Bouilov, L. L.; Zhirnov, V. V.; Kamenev, A. I.; Kovalskij, K. A.; Spitsyn, B. V. *Diamond Relat. Mater.* **1999**, *8*, 369, and references therein.
- (4) (a) Morz, T. J., Jr. *Ceram. Bull.* **1991**, *70*, 849. (b) *Chemistry of Aluminum, Gallium, Indium and Thallium*; Downs, A. J., Ed.; Chapman and Hall: New York, 1993. (c) Pandey, R.; Sutjianto, A.; Seel, M.; Jaffe, J. E. *J. Mater. Res.* **1993**, *8*, 1992. (d) Ruiz, E.; Alvarez, S.; Alemany, P. *Phys. Rev. B: Condens. Matter* **1994**, *94*, 7115. (e) Miwa, K.; Fukumoto, A. *Phys. Rev. B* **1993**, *48*, 789. (f) Ueno, M.; Onodera, A.; Shimomura, O.; Takemura, K. *Phys. Rev. B* **1992**, *45*, 10123. (g) Knudsen, A. K. *Bull. Am. Ceram. Soc.* **1995**, *74*, 97. (h) Timoshkin, A. Y.; Bettinger, H. F.; Schaeffer, H. F., III. *J. Am. Chem. Soc.* **1997**, *119*, 5668. (i) Krupitskaya, R. Y.; Auner, G. W. *J. Appl. Phys.* **1998**, *84*, 2861. (j) Kiehne, G. T.; Wong, G. K. L.; Ketterson, J. B. *J. Appl. Phys.* **1998**, *84*, 5922.
- (5) (a) Schleyer, P. v. R.; Boldyrev, A. I. *J. Chem. Soc., Chem. Commun.* **1991**, 1536. (b) Boldyrev, A. I.; Schleyer, P. v. R. *J. Am. Chem. Soc.* **1991**, *113*, 9045. (c) Boldyrev, A. I.; Simons, J. *J. Am. Chem. Soc.* **1998**, *120*, 7967. (d) Li, X.; Wang, L.-S.; Boldyrev, A. I.; Simons, J. *J. Am. Chem. Soc.* **1999**, *121*, 6033. (e) Li, X.; Zhang, H. F.; Wang, L. S.; Geske, G. D.; Boldyrev, A. I. *Angew. Chem., Int. Ed.* **2000**, *39*, 3630. (f) Wang, L. S.; Boldyrev, A. I.; Li, X.; Simons, J. *J. Am. Chem. Soc.* **2000**, *122*, 7681. (g) Zakrzewski, V. G.; Niessen, von W.; Boldyrev, A. I.; Schleyer, P. v. R. *Chem. Phys. Lett.* **1993**, *174*, 167. (h) Boldyrev, A. I.; Li, X.; Wang, L. S. *Angew. Chem., Int. Ed.* **2000**, *39*, 3307. (i) Li, X.; Zhan, H. J.; Wang, L. S. *Chem. Phys. Lett.* **2002**, *357*, 415. (j) Nayak, S. K.; Khanna, S. N.; Jena, P. *Phys. Rev. B* **1998**, *57*, 3787. (k) Nayak, S. K.; Rao, B. K.; Jena, P.; Li, X.; Wang, L. S. *Chem. Lett.* **1999**, *301*, 379. (l) Boo, B. H.; Liu, Z. J. *Phys. Chem. A* **1999**, *103*, 1250. (m) Andrews, L.; Zhou, M.; Chertihin, G. V.; Bare, W. D.; Hannachi, Y. *J. Phys. A* **2000**, *104*, 1656, and references therein. (n) Leski, B. R.; Castleman, A. W., Jr.; Ashman, C.; Khanna, S. N. *J. Chem. Phys.* **2001**, *114*, 1165. (o) Ling, L.; Song, B.; Cao, P.-L. *J. Mol. Struct.: THEOCHEM* **2005**, *728*, 215. (p) Gou, L.; Wu, H.-S. *Int. J. Quantum Chem.* **2006**, *106*, 1250. (q) Li, X.; Wang, L. S. *Eur. Phys. J. D* **2005**, *34*, 9. (r) Meloni, G.; Sheehan, S. M.; Parsons, B. F.; Neumark, D. M. *J. Phys. Chem. A* **2006**, *110*, 3527. (s) Boris, B.; Boldyrev, A. I.; Li, X.; Wang, L. S. *J. Chem. Phys.* **2006**, *125*, 124305, and references therein.
- (6) (a) Kroto, H. W.; Heath, J. R.; O'Brien, S. C.; Curl, R. F.; Smalley, R. E. *Nature (London)* **1985**, *318*, 162. (b) Kratschmer, W.; Lamb, L. D.; Fostiropoulos, F.; Huffman, D. R. *Nature (London)* **1990**, *347*, 354. (c) Dresselhaus, M. S.; Dresselhaus, G.; Eklund, P. C. *Science of Fullerenes and Carbon Nanotubes*; Academic: San Diego, 1996.
- (7) (a) Guo, B. C.; Kerns, K. P.; Castleman, A. W. *Science* **1992**, *255*, 1411. (b) Cartier, S. F.; Chen, Z. Y.; Walder, G. J.; Sleppy, C. R.; Castleman, A. W., Jr. *Science* **1993**, *260*, 195. (c) Cartier, S. F.; May, B. D.; Castleman, A. W., Jr. *J. Am. Chem. Soc.* **1994**, *116*, 5295. (d) Deng, H. T.; Kerns, K. P.; Castleman, A. W., Jr. *J. Am. Chem. Soc.* **1996**, *118*, 446.
- (8) (a) Li, X.; Wu, H.; Wang, X. B.; Wang, L. S. *Phys. Rev. Lett.* **1998**, *81*, 1909. (b) Dolgounitchcheva, O.; Zakrzewski, V. G.; Ortiz, J. V. *J. Chem. Phys.* **1999**, *111*, 10762. (c) Zheng, W. J.; Thomas, O. C.; Lipka, T. P.; Xu, S. J.; Bowen, K. H., Jr. *J. Chem. Phys.* **2006**, *124*, 144304, and references therein. (d) Khanna, S. N.; Jena, P. *Phys. Rev. Lett.* **1992**, *69*, 1664. (e) Khanna, S. N.; Jena, P. *Phys. Rev. B* **1995**, *51*, 13705. (f) Kurikawa, T.; Takeda, H.; Hirano, M.; Judai, K.; Arita, T.; Nagao, S.; Nakajima, A.; Kaya, K. *Organometallics* **1999**, *18*, 1430.
- (9) The NICS above 0.5 and 1 Å out of the square plane Al₄N[−] (NICS(0.5) = −29.5191, and NICS(1) = −26.0556) describes the aromaticity of Al₄N[−] at the B3LYP/6-311+G(d) level of theory. For the example of NICS see: Schleyer, P. v. R.; Maerker, C.; Dransfeld, A.; Jiao, H.; Hommes, N. J. R. V. E. *J. Am. Chem. Soc.* **1996**, *118*, 6317.
- (10) (a) Peckham, T. J.; Gomez-Elipe, P.; Manners, I. *Metalloenes*, Vol. 2; Togni, A.; Halterman, R. L., Eds.; Wiley-VCH: Weinheim, 1998; p 724. (b) Yang, L. M.; Ding, Y. H.; Sun, C. C. *ChemPhysChem* **2006**, *7*, 2478–2482. (c) Yang, L. M.; Ding, Y. H.; Sun, C. C. *Chem. Eur. J.* **2007**, *13*, 2546–2555. (d) Yang, L. M.; Ding, Y. H.; Sun, C. C. *J. Am. Chem. Soc.* **2007**, *129*, 658–665. (e) Yang, L. M.; Ding, Y. H.; Sun, C. C. *J. Am. Chem. Soc.* **2007**, *129*, 1900–1901. (f) Yang, L. M.; Wang, J.; Ding, Y. H.; Sun, C. C. *Organometallics* **2007**, *26*, 4449. (g) Yang, L. M.; Wang, J.; Ding, Y. H.; Sun, C. C. *J. Phys. Chem. A* **2007**, *111*, 9122–9129. (h) Yang, L. M.; Ding, Y. H.; Tian, W. Q.; Sun, C. C. *Phys. Chem. Chem. Phys.* **2007**, B707898F, ASAP article. (i) Yang, L. M.; Ding, Y. H.; Sun, C. C. *Theor. Chem. Acc.* **2007**, in press.
- (11) (a) Bergeron, D. E.; Castleman, A. W., Jr.; Morisato, T.; Khanna, S. N. *Science* **2004**, *304*, 84–87. (b) Bergeron, D. E.; Roach, P. J.; Castleman, A. W.; Jones, N.; Khanna, S. N. *Science* **2005**, *307*, 231–235.
- (12) (a) Tsuzuki, S.; Honda, K.; Uchimaru, T.; Mikami, M.; Tanabe, K. *J. Am. Chem. Soc.* **2002**, *124*, 104, and references therein. (b) Sinnokrot, M. O.; Valeev, E. F.; Sherrill, C. D. *J. Am. Chem. Soc.* **2002**, *124*, 10887, and references therein. (c) Burley, S. K.; Petsko, G. A. *Science* **1985**, *229*, 23. (d) Hunter, C. A. *Chem. Soc. Rev.* **1994**, *23*, 101. (e) Rebek, J., Jr. *Chem. Soc. Rev.* **1996**, *25*, 255. (f) Felker, P. M.; Maxton, P. M.; Schaeffer, M. W. *Chem. Rev.* **1994**, *94*, 1787.
- (13) (a) Becke, A. D. *J. Chem. Phys.* **1993**, *98*, 5648. (b) Lee, C.; Yang, W.; Parr, R. G. *Phys. Rev. B* **1988**, *37*, 785. (c) Clark, T.; Chandrasekhar, J.; Spitznagel, G. W.; Schleyer, P. v. R. *J. Comput. Chem.* **1983**, *4*, 294. (d) Frisch, M. J.; Pople, J. A.; Binkley, J. S. *J. Chem. Phys.* **1984**, *80*, 3265. (e) Frisch, M. J., et al. *Gaussian03*, Rev. A.1; Gaussian, Inc.: Pittsburgh, PA, 2003. (For full citations, see Supporting Information). (f) MO pictures were made with MOLDEN3.4 program. G. Schaftenaar, MOLDEN3.4, CAOS/ CAMM Center: The Netherlands, 1998.
- (14) (a) Mercero, J. M.; Ugalde, J. M. *J. Am. Chem. Soc.* **2004**, *126*, 3380. (b) Mercero, J. M.; Formoso, E.; Matxain, J. M.; Eriksson, L. A.; Ugalde, J. M. *Chem. Eur. J.* **2006**, *12*, 4495. (c) Urnezus, E.; Brennessel, W. W.; Cramer, C. J.; Ellis, J. E.; Schleyer, P. v. R. *Science* **2002**, *295*, 832. (d) Lein, M.; Frunzke, J.; Frenking, G. *Inorg. Chem.* **2003**, *42*, 2504. (e) Frunzke, J.; Lein, M.; Frenking, G. *Organometallics* **2002**, *21*, 3351. (f) Mercero, J. M.; Matxain, J. M.; Ugalde, J. M. *Angew. Chem., Int. Ed.* **2004**, *43*, 5485. (g) Cheng, L. P.; Li, Q. S. *J. Phys. Chem. A* **2003**, *107*, 2882. (h) Cheng, L. P.; Li, Q. S. *J. Phys. Chem. A* **2005**, *109*, 3182. (i) Guan, J.; Li, Q. S. *J. Phys. Chem. A* **2005**, *109*, 9875.
- (15) (a) Li, J.; Li, X.; Zhai, H. J.; Wang, L. S. *Science* **2003**, *299*, 864. (b) Zhang, H. F.; Stender, M.; Zhang, R.; Wang, C. M.; Li, J.; Wang, L. S. *J. Phys. Chem. B* **2004**, *108*, 12259–12263.
- (16) (a) Bauernschmitt, R.; Ahlrichs, R. *Chem. Phys. Lett.* **1996**, *256*, 454. (b) Gisbergen, S. J. A.; van Kootstra, F.; Schipper, P. R. T.; Gritsenko, O. V.; Snijders, J. G.; Baerends, E. J. *J. Phys. Rev. A* **1998**, *57*, 2556. (c) Matsuzawa, N. N.; Ishitani, A.; Dixon, D. A.; Uda, T. *J. Phys. Chem. A* **2001**, *105*, 4953. (d) The natural charge distribution of the free Al₄N[−] is as follows: N atom carries negative charge: −2.3084 and Al atom carries positive charge: 0.3271 at the B3LYP/6-311+G(d) level.